Growing vortex patches

Darren Crowdy[a] and Jonathan Marshall[b]
Department of Mathematics, Imperial College of Science, Technology and Medicine, 180 Queen's Gate, London SW7 2AZ, United Kingdom

(Received 10 December 2003; accepted 10 May 2004; published online 6 July 2004)

This paper demonstrates that two well-known equilibrium solutions of the Euler equations—the corotating point vortex pair and the Rankine vortex—are connected by a continuous branch of exact solutions. The central idea is to ''grow'' new vortex patches at two stagnation points that exist in the frame of reference of the corotating point vortex pair. This is done by generalizing a mathematical technique for constructing vortex equilibria first presented by Crowdy [D. G. Crowdy, ''A class of exact multipolar vortices,'' Phys. Fluids **11**, 2556 (1999)]. The solutions exhibit several interesting features, including the merging of two separate vortex patches via the development of touching cusps. Numerical contour dynamics methods are used to verify the mathematical solutions and reveal them to be robust structures. The general issue of how simple vortex equilibria can be continued continuously to more complicated ones with very different vortical topologies is discussed. The solutions are examples of exact solutions of the Euler equations involving multiple interacting vortex patches. © *2004 American Institute of Physics.*
[DOI: 10.1063/1.1767771]

I. INTRODUCTION

Point-vortex models and vortex-patch models are by far the most popular and well studied in vortex dynamics.[1,2] Point-vortex models have the advantage of reducing the problem to that of tracking a discrete point set while vortex-patch models reduce the problem to that of tracking a curve (or set of curves). Such mathematical simplifications prove to be of great advantage.

In studying any dynamical system, an important first step is to gain a thorough understanding of the possible equilibrium configurations since they are often attractors in the dynamics. For this reason, the subject of ''vortex statics'' is an important one.[3] One of the very simplest nontrivial point-vortex equilibria is the corotating point vortex pair in which two equal point vortices corotate about the central point of their line of centers. On the other hand, the simplest example of a vortex-patch equilibrium is undoubtedly the Rankine vortex solution[1,2] which describes a circular patch of uniform vorticity in solid-body rotation. In this paper, a vortex patch is understood to be a region of fluid in which the vorticity is a uniform constant.

Point vortices and uniform vortex patches are closely related. The limit in which the radius of a Rankine vortex vanishes while its vorticity tends to infinity in such a way that the circulation is fixed is known to yield a point-vortex solution. At the same time, the idea of desingularizing, or regularizing, a point vortex by smearing out the vorticity to a uniform patch of nonzero area is well known. Dritschel,[4] for example, smeared out the vorticity in the rotating N-polygonal point vortex arrays considered by Thomson[1,2] to find modified equilibria involving N corotating vortex patches. Elcrat and Miller[5] have proved the existence of equilibrium vortex patches close to a stable configuration of point vortices. Converting point vortices to patches, or vice versa, is a common method of producing modified equilibria from existing ones.

Other methods of constructing modified equilibria from any given one have recently been proposed. A given steadily rotating equilibrium of point vortices, for example, often exhibits points of relative rest in a frame of reference corotating with the equilibrium. In the context of point-vortex dynamics, Aref and Vainchtein[6] have proposed the idea of constructing more complicated point-vortex equilibria by ''growing'' new point vortices at any such corotating points. A zero-circulation point vortex is dynamically inactive and can be placed at any such corotating points without affecting the equilibrium. The idea of Aref and Vainchtein[6] is to perform a continuation in the circulation of any such nascent point vortices in an attempt to create new equilibria involving more complicated vortical configurations. While there is no guarantee that such continued solutions exist, in cases where they do, new (and even asymmetric) equilibria can be constructed.

Here, we develop this idea in a natural way and consider the possibility of growing new vortex patches (as opposed to point vortices) at the corotating points of an existing vortical equilibrium. This paper illustrates that this is sometimes possible and an explicit example is presented in detail using perhaps the simplest nontrivial equilibrium—the corotating point-vortex pair. The mathematical construction is based on extensions of ideas originally presented in Crowdy[7] and developed in Crowdy.[8,9] A consequence of the analysis is to show that the corotating point-vortex pair is, in fact, connected by a continuous branch of nontrivial vortex equilibria to the classical Rankine vortex solution. Moreover, the entire

[a]Electronic mail: d.crowdy@imperial.ac.uk
[b]Electronic mail: jonathan.marshall@imperial.ac.uk

branch of solutions is describable in mathematical form by means of analytical formulas (although one of the parameters appearing in these formulas must be determined numerically).

While this result is of theoretical interest in its own right, perhaps more important is the more general question which it provokes concerning how different vortical equilibria, perhaps with very different vortical topologies, might be connected and how a given equilibrium might be ''continued,'' in a continuous fashion, to a more complicated one. The explicit example presented here starts with a vorticity distribution consisting of a simple two-point set. This is continued, continuously, to a distribution consisting of a hybrid combination of two-point vortices and two-vortex patches. The latter configuration is then smoothly continued to a distribution involving four-vortex patches which, finally, coalesce into a single isolated Rankine vortex. Being inherently nonlinear, the steady Euler equation is renowned for being difficult to solve. For this reason, a thorough understanding of how complicated vortical equilibria can be systematically constructed by continuous deformations of simpler ones is desirable and is discussed in Sec. VIII.

It should be remarked that the class of solutions involve vortex patches that are in pure solid-body rotation and are not the only possible rotating equilibria consisting of two patches and two-point vortices. More general solutions in which the fluid in the vortex patches has a nontrivial irrotational component are also possible, but it is likely that this more general class is not describable in analytical form.

II. THE COROTATING POINT-VORTEX PAIR

Consider two-point vortices, each of circulation $2\pi\omega$, initially at points $(0,\pm 1)$. Introducing the usual complex coordinate $z=x+iy$, the associated instantaneous complex potential $w(z)$ for this flow is

$$w(z)=-i\omega\ln(z-i)-i\omega\ln(z+i). \tag{1}$$

It is straightforward to show that such a configuration rotates about the origin with angular velocity equal to $\omega/2$. In a frame of reference corotating with this angular velocity, the configuration is stationary and the complex velocity field $u-iv$ has the form

$$u-iv=\frac{dw}{dz}=-i\omega\left(\frac{1}{z-i}+\frac{1}{z+i}-\frac{\bar{z}}{2}\right). \tag{2}$$

A simple calculation shows that this velocity field has stagnation points at $z=0,\pm\sqrt{3}$. Equivalently, because these points are stagnation points in a corotating frame, one might equally well refer to these as ''corotating points'' following Aref and Vainchtein[6] (see also Morton[10]). In the following section, it is shown how to grow two new vortex patches at the corotating points located at $z=\pm\sqrt{3}$.

III. MATHEMATICAL CONSTRUCTION

Crowdy[8,9] has demonstrated the theoretical advantages of considering streamfunctions of the form

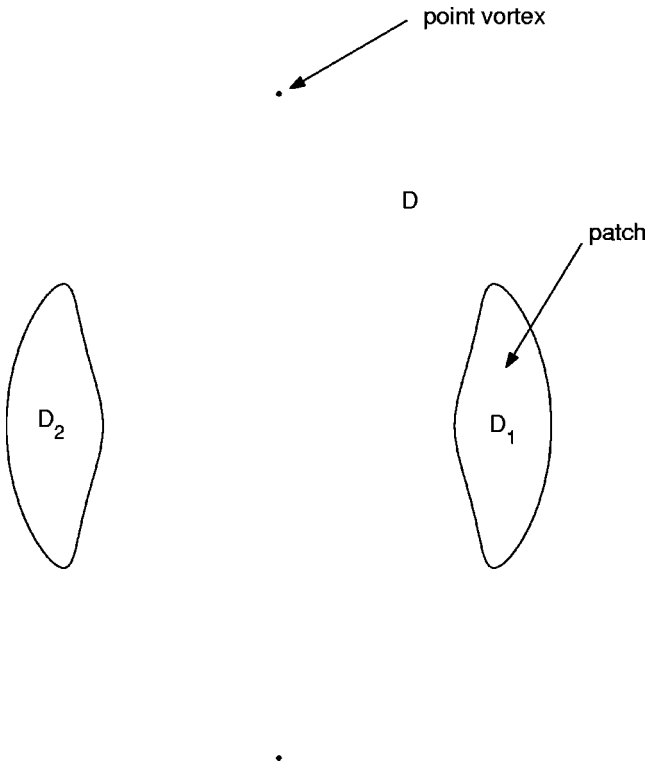

FIG. 1. Schematic illustrating the vortex configuration of interest. Two-point vortices are at $(0,\pm 1)$ while two rotationally symmetric uniform vortex patches are located on the positive and negative real axis.

$$\psi=\begin{cases}\dfrac{\omega}{4}\left(z\bar{z}-\displaystyle\int^{z}S(z')dz'-\int^{\bar{z}}\bar{S}(z')dz'\right) & z\in D\\ 0 & z\notin D\end{cases}, \tag{3}$$

where D is some fluid region and $S(z)$ is the Schwarz function[11] of the boundary curve ∂D. For certain special choices of fluid domain D, such a streamfunction can represent an equilibrium solution of the Euler equation. Moreover, in many cases, these special classes of domains can be parametrized using conformal mappings thus effectively leading to exact solutions of the Euler equation.

This constructive method appears to be quite general, and we will use a variant of it here. Consider a configuration in which, in addition to the two-point vortices at $z=\pm i$, two-vortex patches are located symmetrically on the positive and negative real axis. A schematic is shown in Fig. 1. The irrotational fluid region containing the two-point vortices is denoted D, the two-vortex patches are denoted D_1 and D_2. Let the boundaries of the two patches be ∂D_1 and ∂D_2. It will be assumed that the vortex patches have the same angular velocity $\omega/2$ as the rotating point vortex configuration and, moreover, are in pure solid-body rotation about the origin. The uniform vorticity of each patch is therefore ω and the assumption of solid-body rotation implies that, in the corotating frame, the fluid inside the two patches is stagnant.

Now pose that the streamfunction of the flow, in a frame of reference corotating with angular velocity $\omega/2$, is of the form (3) where $S(z)$ is now the Schwarz function (if it exists) of both boundaries of D, i.e., ∂D_1 and ∂D_2. Recall that the vorticity is given by $-4\psi_{z\bar{z}}$ where subscripts denote par-

tial differentiation. This means that, in the corotating frame, the vorticity inside D associated with the streamfunction (3) is a uniform constant. Note also that the function $S(z)$, which is locally analytic in annular neighborhoods of both ∂D_1 and ∂D_2, must satisfy

$$S(z)=\overline{z} \tag{4}$$

on both ∂D_1 and ∂D_2. If there are just two-point vortices in D, it is clear that an additional restriction on the function $S(z)$ is that it must only have two simple poles in D.

The associated velocity field is

$$u-iv\equiv 2i\psi_z=\frac{i\omega}{2}[\overline{z}-S(z)]. \tag{5}$$

If $S(z)$ satisfies (4) on ∂D_1 and ∂D_2, it is easy to verify that this streamfunction satisfies the kinematic and dynamic boundary conditions on both boundaries ∂D_1 and ∂D_2 of D. The kinematic boundary condition is that both ∂D_1 and ∂D_2 are streamlines, the dynamic boundary condition is that the velocity field must vanish everywhere on these boundaries in order to be continuous with the stagnant flow inside the patches. Continuity of velocity on the boundary of a steady vortex patch implies that the hydrodynamic pressures are continuous.[1]

IV. CONFORMAL MAPPING

As in Crowdy,[7,8] the most effective way to construct the relevant fluid domains D is to employ conformal mapping techniques. Here, D is an unbounded doubly connected domain. The Riemann mapping theorem guarantees that any such domain can be conformally mapped from some annulus $\rho<|\zeta|<1$ in a parametric ζ plane. The parameter ρ relevant to any given domain must be determined as part of the problem.

Let the conformal map be $z(\zeta)$ and suppose that the circle $|\zeta|=1$ maps to ∂D_1 while $|\zeta|=\rho$ maps to ∂D_2. Note that on ∂D_1,

$$S(z)=\overline{z}=\overline{z(\zeta)}=\overline{z}(\zeta^{-1}), \tag{6}$$

where we have used the fact that $\overline{\zeta}=\zeta^{-1}$ on $|\zeta|=1$ and the conjugate function $\overline{z}(\zeta)$ is defined by

$$\overline{z}(\zeta)=\overline{z(\overline{\zeta})}. \tag{7}$$

Note also that on ∂D_2,

$$S(z)=\overline{z}=\overline{z(\zeta)}=\overline{z}(\rho^2\zeta^{-1}), \tag{8}$$

where we have used the fact that $\overline{\zeta}=\rho^2\zeta^{-1}$ on $|\zeta|=\rho$. In order for (6) and (8) to be consistent it is clear that the conformal map must satisfy

$$\overline{z}(\rho^2\zeta)=\overline{z}(\zeta) \tag{9}$$

for all ζ.

V. EXACT SOLUTIONS

Consider now the conformal mapping given by

$$z(\zeta)=R\frac{P(-\zeta\sqrt{\rho}^{-1})P(-\zeta\sqrt{\rho})P(\zeta\sqrt{\rho})}{P(\zeta\sqrt{\rho}^{-1})P(\zeta\sqrt{\rho}e^{i\theta})P(\zeta\sqrt{\rho}e^{-i\theta})}, \tag{10}$$

where R and θ are some real parameters and the special function $P(\zeta)$ is defined as

$$P(\zeta)=(1-\zeta)\prod_{k=1}^{\infty}(1-\rho^{2k}\zeta)(1-\rho^{2k}\zeta^{-1}). \tag{11}$$

This is the same special function used by Crowdy[9] to construct exact solutions for annular arrays of vortices. It is related to the first Jacobi theta function.[12] Note that the map has a simple pole at the point $\zeta=\sqrt{\rho}$ which therefore maps to physical infinity, while it has a zero at $\zeta=-\sqrt{\rho}$ which therefore maps to $z=0$. The conformal map (10) depends on just three real parameters R, ρ, and θ.

It is straightforward to show, by use of its definition (11), that $P(\zeta)$ satisfies the functional relations

$$P(\rho^2\zeta)=-\zeta^{-1}P(\zeta),$$
$$P(\zeta^{-1})=-\zeta^{-1}P(\zeta). \tag{12}$$

These relations (12) are all that are needed to verify directly that $z(\zeta)$ satisfies

$$z(\rho\zeta^{-1})=-z(\zeta), \tag{13}$$

which implies that for every point ζ on the unit circle mapping to z_1, say, there is a point $\rho\zeta^{-1}$ on the ρ-circle mapping to $-z_1$. This means that the mapping produces two rotationally symmetric vortex patches, as required. Also, (12) can be used to verify directly that $z(\zeta)$ satisfies the requirement given in (9) which is essentially the condition that the Schwarz functions of the two separate boundaries ∂D_1 and ∂D_2 are the same. Finally, noting that

$$S(z)=\overline{z}(\zeta^{-1})$$
$$=R\frac{P(-\zeta^{-1}\sqrt{\rho}^{-1})P(-\zeta^{-1}\sqrt{\rho})P(\zeta^{-1}\sqrt{\rho})}{P(\zeta^{-1}\sqrt{\rho}^{-1})P(\zeta^{-1}\sqrt{\rho}e^{i\theta})P(\zeta^{-1}\sqrt{\rho}e^{-i\theta})}, \tag{14}$$

it is clear that $S(z)$ has just two simple poles in the annulus $\rho<|\zeta|<1$, at the points $\zeta=\sqrt{\rho}e^{i\theta},\sqrt{\rho}e^{-i\theta}$. This means that $S(z)$ has just two simple poles in D at the corresponding conformally mapped points $z(\sqrt{\rho}e^{i\theta})$ and $z(\sqrt{\rho}e^{-i\theta})$, again as required. The scaling parameter R is fixed by insisting that the two-point vortices are at $\pm i$ which is equivalent to the equation

$$i=z(\sqrt{\rho}e^{i\theta}). \tag{15}$$

The conformal map (10) therefore satisfies *almost* all of the requirements for a mapping to an appropriate equilibrium domain D. The only outstanding condition is to ensure that the two-point vortices are stationary under the effects of the local non-self-induced velocity field. By symmetry, it is only necessary to ensure that this condition of stationarity is satisfied at one of the point vortices. Substituting (10) and (14)

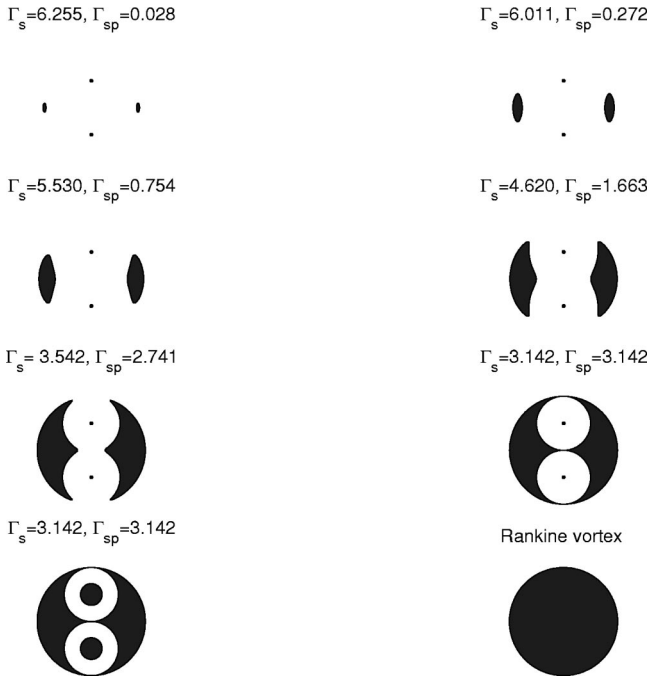

FIG. 2. A continuous branch of rotating vortex arrays connecting the corotating point-vortex pair to the Rankine vortex. The figures illustrate the "growing" of two-vortex patches at the two stagnation points (at $\pm\sqrt{3}$ in the corotating frame) of the corotating point-vortex pair. The sixth figure is the limiting state of the solution (10) where $\rho=\rho_{crit}$ and where the two patches develop cusps and touch at three distinct points enclosing circular irrotational regions centered on the point vortices. The last two figures illustrate the desingularization of the point vortices to form a single Rankine vortex. The circulations Γ_s and Γ_{sp} are also shown.

into (5) one obtains a formula for the complex velocity field, in the corotating frame, as a function of ζ and $\overline{\zeta}$. This is

$$u-iv=\frac{i\omega R}{2}\left(\frac{P(-\overline{\zeta}\sqrt{\rho}^{-1})P(-\overline{\zeta}\sqrt{\rho})P(\overline{\zeta}\sqrt{\rho})}{P(\overline{\zeta}\sqrt{\rho}^{-1})P(\overline{\zeta}\sqrt{\rho}e^{i\theta})P(\overline{\zeta}\sqrt{\rho}e^{-i\theta})}-\frac{P(-\zeta^{-1}\sqrt{\rho}^{-1})P(-\zeta^{-1}\sqrt{\rho})P(\zeta^{-1}\sqrt{\rho})}{P(\zeta^{-1}\sqrt{\rho}^{-1})P(\zeta^{-1}\sqrt{\rho}e^{i\theta})P(\zeta^{-1}\sqrt{\rho}e^{-i\theta})}\right). \tag{16}$$

On use of the conformal mapping function it can be shown that, as $z\to i$, the velocity field (16) locally has the form

$$u-iv=-\frac{i\Gamma_s}{2\pi(z-i)}+V+o(1), \tag{17}$$

where Γ_s is the circulation of the point vortex at $z=i$ and V is the local non-self-induced velocity. The condition that the two-point vortices are stationary under the non-self-induced velocity field is equivalent to $V=0$. The Appendix gives expressions for Γ_s and the condition that $V=0$ in terms of the conformal mapping parameters. By the symmetry, this condition also ensures that the vortex at $z=-i$ is stationary. As seen in the Appendix, this equation is independent of R (which is simply a scaling parameter) but depends only on ρ and θ. By applying Newton's method to this equation, we have found that it can be solved numerically for θ for given ρ in the interval

$$\rho\in[0,\rho_{crit}], \tag{18}$$

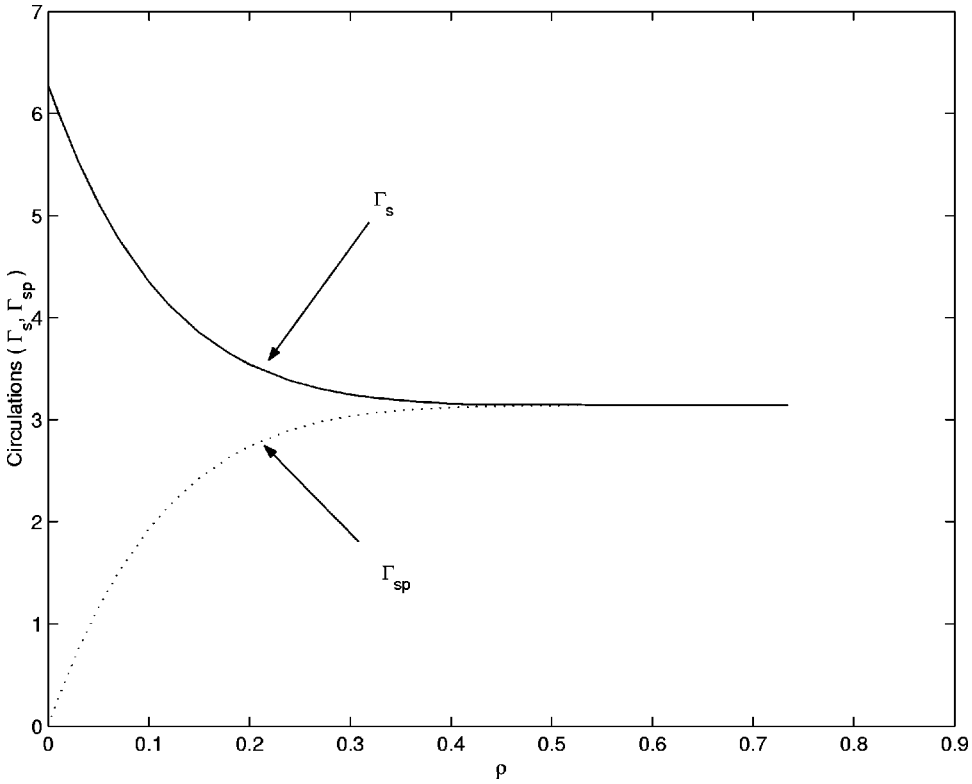

FIG. 3. Graph of satellite patch circulations Γ_{sp} and satellite point-vortex circulations Γ_s against ρ. The sum $\Gamma_s+\Gamma_{sp}$ is found to equal 2π for all values of ρ. As $\rho\to\rho_{crit}$, Γ_s, $\Gamma_{sp}\to\pi$.

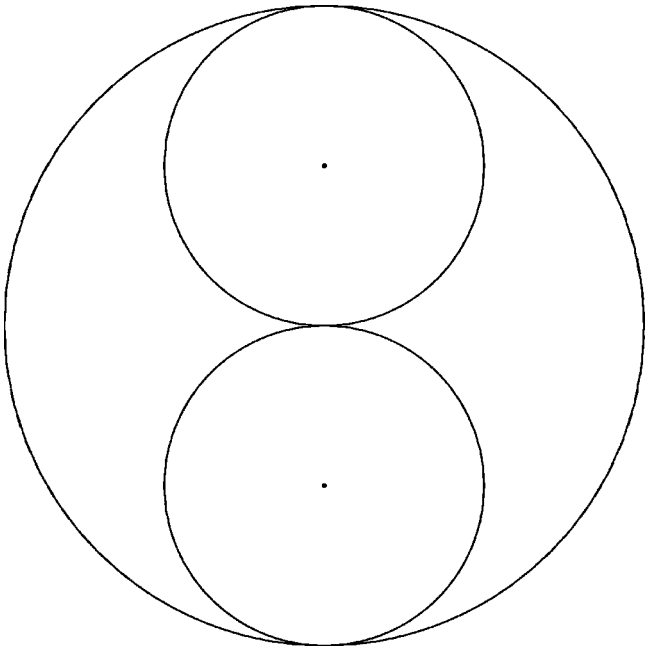

FIG. 4. Critical configuration for two satellite patches and two satellite point vortices for $\rho=\rho_{crit}=0.735$ (drawn in solid lines) shown with the three circles $|z\pm i|=1$ and $|z|=2$ superposed (drawn with dashed lines). The solid and dashed curves are indistinguishable. In this critical case, the circulation of each satellite patch is π, as is the circulation of each satellite point vortex.

where ρ_{crit} yields a limiting configuration to be discussed in the following section. The solution to this equation is very straightforward since it is a Newton iteration on just a single unknown parameter.

VI. CHARACTERIZATION OF THE SOLUTIONS

The conformal map (10), with the three parameters R, ρ, and θ constrained by the two conditions of stationarity of the point vortices and the normalization (15) yield a continuous one-parameter family of two-patch equilibria. Without loss of generality, we set $\omega=1$. In the limit $\rho\to 0$, it is found that the two-vortex patches become invisibly small and essentially disappear at $z=\pm\sqrt{3}$ in this limit. This is precisely the location of the corotating points in the pure point-vortex configuration discussed in Sec. II. For this reason, the constructive procedure just described essentially effects the job of growing two-vortex patches at these corotating points.

As ρ increases, so does the size of each vortex patch. Figure 2 shows several configurations for different values of ρ. Different values of ρ correspond to different values of the circulations of both the point vortices and the patches. Let Γ_s denote the point-vortex circulations and let Γ_{sp} denote the circulation of each of the vortex patches. The expression (16) can be used to derive analytical expressions for Γ_s and Γ_{sp} in terms of the conformal mapping parameters. Figure 2 annotates each configuration with the corresponding values of these circulations. When $\rho\to 0$, Γ_{sp} tends to zero (because it is proportional to the patch area). A superposed graph of Γ_s and Γ_{sp} is shown in Fig. 3 and displays a surprising feature. To within numerical accuracy (in the solution of the stationarity condition for θ given a value of ρ), it is found that all the equilibrium configurations satisfy

$$\Gamma_s+\Gamma_{sp}=2\pi. \tag{19}$$

Thus, while the values of Γ_s and Γ_{sp} both change with ρ, their sum remains constant. We can offer no explanation for this unexpected result.

Perhaps equally surprising is the nature of the limiting configuration as $\rho\to\rho_{crit}=0.735$. This is shown in the sixth diagram of Fig. 2. In this limiting state the two-vortex patches touch at three distinct points, the points of contact taking the form of three cusp singularities in the patch boundaries. As $\rho\to\rho_{crit}$, the curvature of the near cusps gets larger as the distance between corresponding near cusps on the two-vortex patches gets smaller. At $\rho=\rho_{crit}$, within numerical accuracy, it is found that the patches touch and enclose two exactly circular regions of irrotational fluid with the point vortices located at their centers. To test this, Fig. 4 shows the critical configuration superposed with the three circles $|z\pm i|=1$ and $|z|=2$. The boundaries of the limiting configuration are indistinguishable from these three circles. It was also noticed that in the limiting configuration, the values of Γ_s and Γ_{sp} become equal. By (19), they both tend to π. This can be seen clearly in Fig. 3.

This feature of the limiting two-patch solutions suggests that the class of solutions can be continued, in a continuous fashion, even past this limiting state. In view of the fact that the streamlines around the point vortices are exactly circular, the two-point vortices can be desingularized in the usual way and replaced by two Rankine vortices (with the same total circulation as the original point vortices) but with gradually increasing radius r. If ω_r denotes the vorticity of a Rankine vortex of radius r and total circulation π then

$$\omega_r=\frac{1}{r^2}. \tag{20}$$

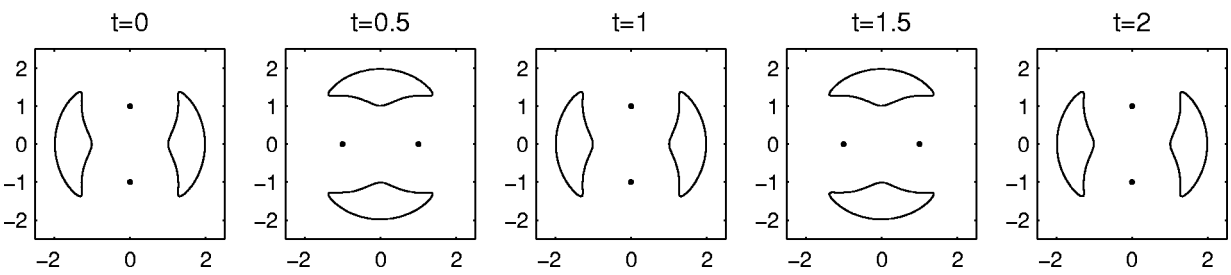

FIG. 5. Contour dynamics simulation of a single revolution of the equilibrium shown in the fourth figure of Fig. 2 with $\Gamma_s=4.620$, $\Gamma_{sp}=1.663$.

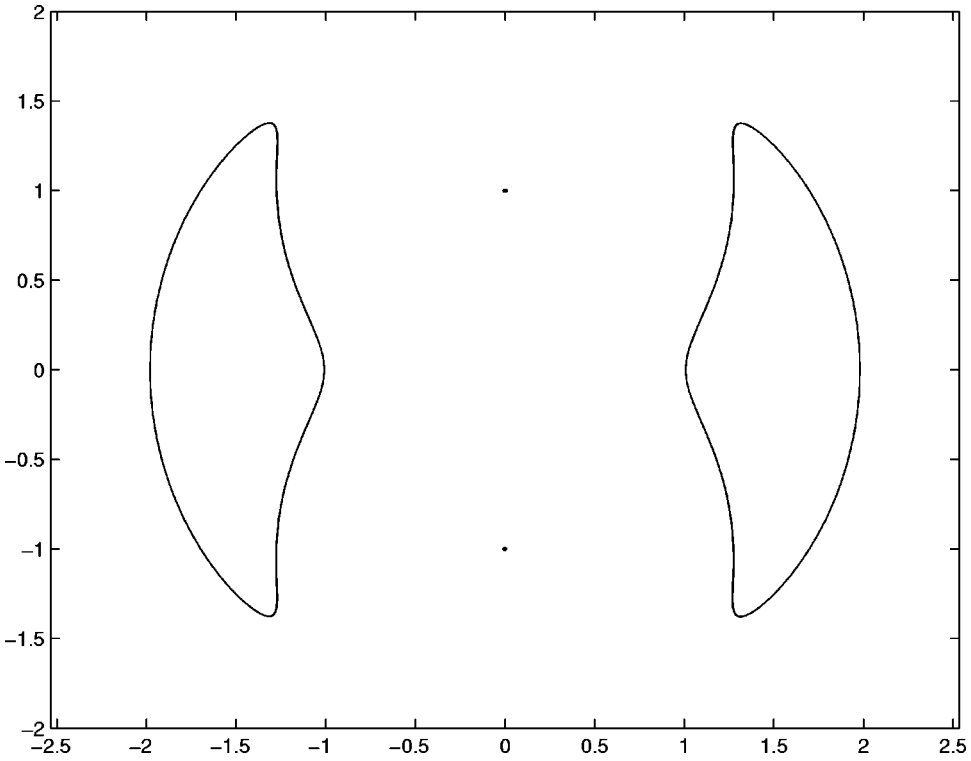

FIG. 6. Superposition of the initial configuration and final configurations after 10 turnover times (i.e., $t=20$) as computed by contour dynamics. The curves sit on top of each other. The initial configuration is the equilibrium shown in the fourth diagram of Fig. 2.

The value of $r \geqslant 0$ is arbitrary provided it is less than, or equal, to unity which is where the enclosed Rankine vortices meet the circular boundaries of the satellite patches. The seventh diagram in Fig. 2 shows the configuration for $r=0.4$. Indeed when $r=1$, by the previously observed fact that the limiting circulation of Γ_s is π, the uniform vorticity of the enclosed circular Rankine vortices tends exactly to the value of the uniform vorticity of the satellite vortex patches implying that, when $r=1$ then $\omega_r=1$ by (20) and the equilibrium essentially becomes a single circular Rankine vortex of radius 2, uniform vorticity $\omega=1$, and total circulation 4π.

Overman[13] showed that points of nonanalyticity in the boundary of a steady vortex patch can either be right-angled corners or cusps. It is known that two corotating vortex patches reach a limiting configuration at which they touch at the same time as a corner develops in the boundary of each patch. Saffman and Szeto[14] and Kamm[15] have investigated such problems. The equilibrium solutions found here exhibit the feature of two equal corotating vortex patches touching (in this case, simultaneously at three distinct points) as the boundaries of the two patches develop cusps, as opposed to corners. The presence of the straining flow due to the point vortices seems to induce this occurrence. This appears to be an example of a limiting equilibrium exhibiting touching cusps. Note that, owing to the presence of these cusps (which have infinite curvature), it is likely that the limiting states would be challenging to compute using any numerical scheme which relies on a discretization of the patch boundaries. The existence of a closed-form formulas for the solutions is therefore of great value.

VII. CONTOUR DYNAMICS SIMULATION

As a check on the mathematical solutions, the contour surgery code of Dritschel[16] for computing the evolution of vortex patches was modified to include the effect of two-point vortices interacting with the patches. This code was initialized using the equilibrium configurations just derived in order to check that they simply rotate without change of form under the dynamics of the Euler equation. Figure 5 shows snapshots of the evolution of the equilibrium in the fourth diagram of Fig. 2 during a single turnover time. Here, time has been rescaled with respect to 2π so, since $\omega=1$ so that the angular velocity is 1/2, then $t=2$ corresponds to a

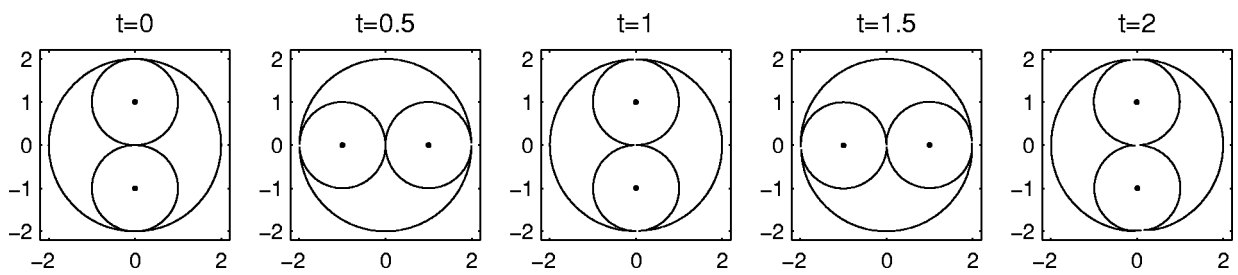

FIG. 7. Contour dynamics simulation of a single revolution of the critical equilibrium.

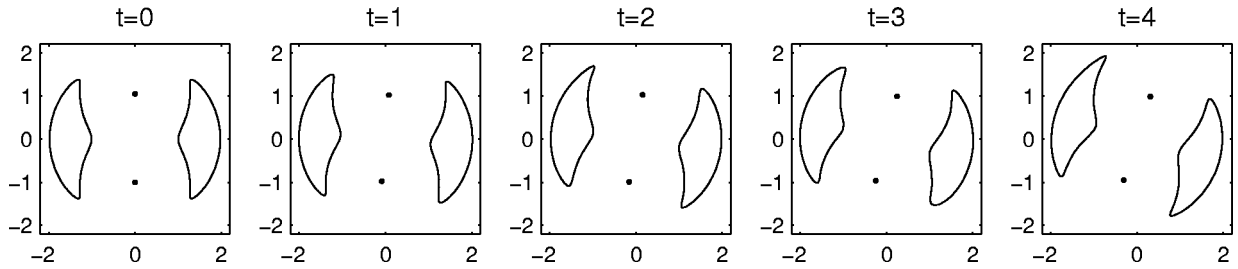

FIG. 8. Contour dynamics simulation of a perturbed equilibrium. The upper point vortex in the equilibrium of the fourth figure of Fig. 2 is displaced upwards by 0.05. The configuration is robust, but its overall angular velocity of rotation is affected.

single revolution of the array. The snapshots are taken at $t=0.5,1,1.5$ and $t=2$ and, indeed, these are clearly found to correspond to quarter revolutions of the configuration. As an additional check, Fig. 6 features a superposition of the initial condition and the final configuration after 10 turnover times (i.e., at $t=20$). Within numerical errors associated with the simulation, the initial condition is verifiably an equilibrium of the equations. Figure 7 shows a simulation of a single revolution of the critical case in which the two patches touch. This too appears to be a robust equilibrium of the equations even though the numerical evolution of the cusp regions of the interface is a little unsteady. It should be mentioned that, owing to the presence of these high curvature regions, a large number of points must be given in the initial conditions for the contour dynamics simulation in this case.

The preceding calculations also suggest that the equilibria might well be linearly stable since if unstable, growth of any small numerical inaccuracies might be expected to destabilize the array after sufficiently long times. A detailed investigation of the stability properties of this class of solutions remains to be performed, however, some preliminary investigations using contour dynamics suggests that the equilibria are robust structures. Figure 8 shows the initial configuration given in the fourth diagram of Fig. 2 but perturbed by displacing the upper point vortex vertically upwards by a distance 0.05. The overall structure remains robust but the angular velocity of rotation is affected. After two revolutions of the unperturbed equilibrium, the configuration has not returned to its original orientation but is displaced through some angle.

As a check on the equilibria constructed by desingularizing the point vortices to Rankine vortices, Fig. 9 shows a contour dynamics simulation of two revolutions of the critical configuration in which the two-point vortices are each replaced by a radius 1/2 Rankine vortex each of vorticity 4. Similarly, Fig. 10 shows a case in which the point vortices are replaced by Rankine vortices of different radii: the upper point vortex is replaced by a Rankine vortex of radius 2/3 and vorticity 9/4 while the lower point vortex is replaced by a Rankine vortex of radius 1/3 and vorticity 9. These simulations corroborate the fact that the vortex configurations are indeed equilibria of the Euler equation.

VIII. DISCUSSION

This paper has demonstrated that the corotating point-vortex pair can be continuously deformed, through a series of equilibria describable using exact mathematical formulas, to the classical Rankine vortex. This has been done by the device of growing two new vortex patches at the corotating points at $z=\pm\sqrt{3}$ of the corotating point-vortex pair.

It should be noted that, as in the point-vortex case considered by Aref and Vainchtein,[6] the success of growing patches at corotating points is not guaranteed. Indeed, in the present example, one could contemplate adapting the same methods used here to grow a new central vortex patch at the corotating point at $z=0$ instead of at $z=\pm\sqrt{3}$. However, this attempt would fail as can be concluded immediately from the fact that such a generalized equilibrium would fall within the class of equilibria consisting of a central vortex patch surrounded by N satellite point vortices considered recently by Crowdy.[8] In the latter study, it was found that equilibrium solutions of this kind can be found for all $N\geqslant 3$ but the case $N=2$ does not yield solutions.

Remarkably, using numerical methods, Cerretelli and Williamson[17] have recently found a completely distinct branch of equilibria connecting the corotating point vortex pair to the Rankine vortex. Instead of growing new vortex

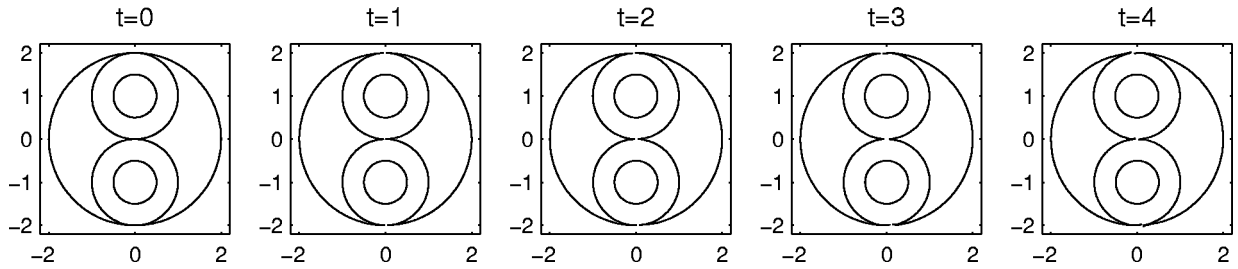

FIG. 9. Contour dynamics simulation of two revolutions of the continued critical equilibrium in which the two-point vortices are replaced by two Rankine vortices each of radius 0.5.

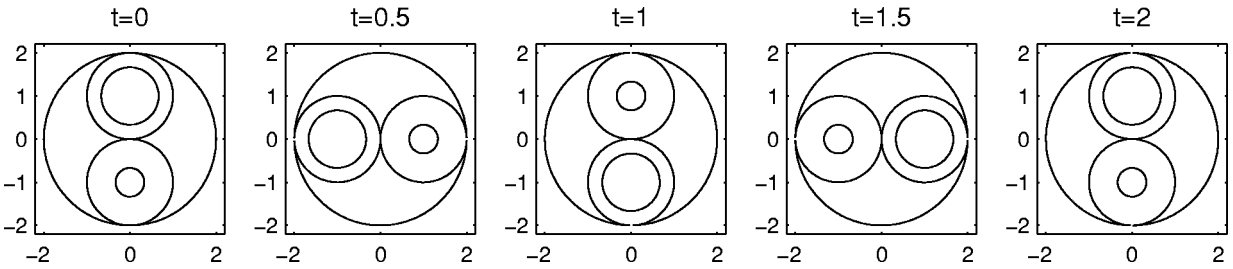

FIG. 10. Contour dynamics simulation of a single revolution of the continued critical equilibrium in which the upper point vortex is replaced by a Rankine vortex of radius 2/3 and vorticity 9/4 while the lower point vortex is replaced by a Rankine vortex of radius 1/3 and vorticity 9.

patches at the corotating points and then later desingularizing the point vortices as done here, the latter authors' approach is to start by desingularizing the two corotating point vortices by replacing them with two finite-area patches. The area of the two (noncircular) patches is gradually increased until the patches touch. Thereafter, Cerretelli and Williamson[17] continue the class of equilibria even beyond this (apparently limiting) state to construct a class of simply connected patch equilibria variously dubbed ''dumb-bells'' and ''sausages'' before the truly limiting ''cat's-eye'' state is reached. En route to this limiting state, the patch becomes a Kirchhoff ellipse which, it is well-known,[1,2] can be continuously deformed (through a sequence of equilibrium ellipses of gradually increasing aspect ratio) back to the circular Rankine vortex. By this path of solutions, the corotating point-vortex pair is again continuously connected to the classical Rankine vortex.

All this evidence suggests powerful possibilities for the future construction of new vortical equilibria based on combined point-vortex and vortex-patch models. By procedures such as (i) the desingularization of point vortices to uniform vortex patches (or vice versa), (ii) the growing of new point vortices at corotation points of existing equilibria as done recently by Aref and Vainchtein,[6] (iii) the growing of new vortex patches at corotation points of existing equilibria as done here, and (iv) the smooth continuation of touching vortex patches to a merged equilibrium as done here and recently by Cerretelli and Williamson,[17] it appears that even basic equilibria with simple vorticity distributions can be continuously continued to more complicated ones with more elaborate vortical topology.

In general, any such continuations must be performed using numerical methods. However, it appears that there exist special cases where exact solutions can be identified. Exact solutions of the steady Euler equation are rare, yet consideration of streamfunctions of the form (3) seems to be unusually successful in producing them as evinced both here and in previous studies.[7–9] Moreover, the resulting solutions appear to have a number of surprising characteristics that have yet to be explained. This is left for future work as the potential of the streamfunction (3) is examined further.

Finally, we mention that the two-patch solutions herein are examples of exact solutions of the Euler equations involving more than one vortex patch. The possibility of extending the general methods to find equilibria involving more than two vortex patches is intriguing but involves the theory of conformal mappings of multiply connected domains. In the doubly connected case considered here, the mappings have been constructed by implicit use of the well-developed theory of elliptic functions [manifested in the use of $P(\zeta)$ which is related to Jacobi theta functions[12]]. For more than two patches, the situation becomes much more challenging and details remain to be worked out. Finally, another interesting generalization is to the case where vortex patches are grown at the corotation points of a corotating point-vortex pair with different strengths, however, we have not studied this case in any detail.

ACKNOWLEDGMENTS

This work is partially supported by a grant from EPSRC in the United Kingdom. J.M. acknowledges the support of an EPSRC studentship.

APPENDIX: THE STATIONARITY CONDITION

The velocity field associated with the exact solutions is (16) which, near $\zeta=\alpha=\sqrt{\rho}e^{i\theta}$ can be written in the form

$$u-iv=\frac{i\omega R}{2}\left(\frac{A(\zeta)}{\zeta-\alpha}+B(\overline{\zeta})\right), \tag{A1}$$

where $A(\zeta)$ is analytic at $\zeta=\alpha$ and where explicit formulas for $A(\zeta)$ and $B(\overline{\zeta})$ can be derived from (16).

Let z_1 denote the position of the point vortex on the imaginary axis. Then $z_1=z(\alpha)$ and

$$z-z_1=z_\zeta(\alpha)(\zeta-\alpha)+\frac{z_{\zeta\zeta}(\alpha)}{2}(\zeta-\alpha)^2+\cdots \tag{A2}$$

so that, with some manipulations, we deduce that

$$\frac{1}{\zeta-\alpha}=\frac{z_\zeta(\alpha)}{z-z_1}+\frac{z_{\zeta\zeta}(\alpha)}{2z_\zeta(\alpha)}+O(z-z_1). \tag{A3}$$

It follows that the circulation Γ_s of the point vortex is

$$\Gamma_s=-\pi\omega RA(\alpha)z_\zeta(\alpha) \tag{A4}$$

while the stationarity condition $V=0$ is equivalent to

$$A_\zeta(\alpha)+A(\alpha)\frac{z_{\zeta\zeta}(\alpha)}{2z_\zeta(\alpha)}+B(\overline{\alpha})=0. \tag{A5}$$

[1]P. G. Saffman, *Vortex Dynamics* (Cambridge University Press, Cambridge, 1992).
[2]P. K. Newton, *The N-vortex Problem* (Springer, New York, 2001).
[3]H. Aref, P. K. Newton, M. A. Stremler, T. Tokieda, and D. L. Vainchtein, ''Vortex crystals,'' Adv. Appl. Mech. **39**, 1 (2002).
[4]D. G. Dritschel, ''The stability and energetics of corotating uniform vortices,'' J. Fluid Mech. **157**, 95 (1985).
[5]A. R. Elcrat and K. G. Miller, ''Rearrangements in steady multiple vortex flows,'' Commun. Partial Differ. Equ. **20**, 1481 (1995).
[6]H. Aref and D. L. Vainchtein, ''Point vortices exhibit asymmetric equilibria,'' Nature (London) **392**, 769 (1998).
[7]D. G. Crowdy, ''A class of exact multipolar vortices,'' Phys. Fluids **11**, 2556 (1999).
[8]D. G. Crowdy, ''Exact solutions for rotating vortex arrays with finite-area cores,'' J. Fluid Mech. **469**, 209 (2002).
[9]D. G. Crowdy, ''On the construction of exact multipolar equilibria of the two-dimension Euler equations,'' Phys. Fluids **14**, 257 (2002).
[10]W. B. Morton, ''On some permanent arrangements of parallel vortices and their points of relative rest,'' Proc. R. Ir. Acad., Sect. A **41**, 94 (1933).
[11]P. Davis, *The Schwarz Function and Its Applications*, Carus Mathematical Monographs (The Mathematical Association of America, Washington, DC, 1974).
[12]M. Abramovitz and I. Stegun, *Handbook of Mathematical Functions* (Dover, New York, 1965).
[13]E. A. Overman, ''Steady state solutions of the Euler equation in two dimensions. II. Local analysis of limiting V-states,'' SIAM (Soc. Ind. Appl. Math.) J. Appl. Math. **46**, 765 (1986).
[14]P. G. Saffman and R. Szeto, ''Equilibrium shapes of a pair of equal uniform vortices,'' Phys. Fluids **23**, 2339 (1980).
[15]J. R. Kamm, ''Shape and stability of two-dimensional vortex regions,'' Ph.D. thesis, Caltech, Pasadena, CA, 1987.
[16]D. Dritschel, ''Contour surgery: a topological reconnection scheme for extended interactions using contour dynamics,'' J. Comput. Phys. **77**, 511 (1988).
[17]C. Cerretelli and C. H. K. Williamson, ''A new family of uniform vortices relating to vortex configurations before merging,'' J. Fluid Mech. **493**, 219 (2003).